Protection of 3D Objects against Illegal Photography Using Optical Watermarking Technique with Spatially Modulated Illumination

Abstract -- We present a new technique that protects the copyrights or portrait rights of 3D objects such as sculptures, bodies, merchandise, and even human with optical watermarking, which is produced by spatially modulated illumination. Although the previous study revealed that the optical watermarking technique could prevent objects from being illegally photographed without protection, the technique could only be applied to 2D objects. The largest problem to be solved in extending this technique to the case of 3D objects is to compensate for geometrical distortion. We solved this problem by introducing rectangular mesh fitting and a technique of "bilinear interpolation" based on the four nearest points. We conducted experiments in which we projected optical watermarking onto the surface of a globe and a model of the human face, and evaluated the accuracy of extracted data. The results were almost 100% in both cases when a Discrete Cosine Transform (DCT) and a Walsh-Hadamard Transform (WHT) were used as methods of embedding watermarks.

I. INTRODUCTION

Techniques of digital watermarking have been widely recognized in recent years as methods of protecting the copyrights of digital image content that is increasingly being distributed throughout the Internet or other media [1]-[3]. For example, digital watermarking is embedded in digital data before it is printed to protect paper images [4]-[5]. This is the same as for other types of digital media, i.e., digital watermarking has to be embedded before the image content

itself distributed. However, this method cannot prevent photographs of valuable paintings from being illegally taken with digital cameras, which have been exhibited at museums and galleries.

We have proposed a novel technology that can prevent the illegal use of images of objects that do not have watermarking. This technique uses illumination that contains invisible watermarking. As the illumination for objects contains watermarking, the images of objects taken by cameras also contain watermarking and this can be extracted by image processing. We carried out experiments using a Walsh-Hadamard Transform (WHT) and a Discrete Cosine Transform (DCT) as methods of embedding the watermarking information and showed that watermarking data were read out from photographed image data with almost 100% accuracy when optical watermarking was projected onto pictures.

One of most important features of this technology is that it can be used for 3D objects like sculptures in museums, merchandise in stores, or even human bodies. If a watermarking image is projected onto such a 3D object, the captured watermarking images usually contain some geometrical and other distortions because the surface is not always flat. If such distortions can be rejected from captured image data, the embedded digital watermarking can be extracted like it is when

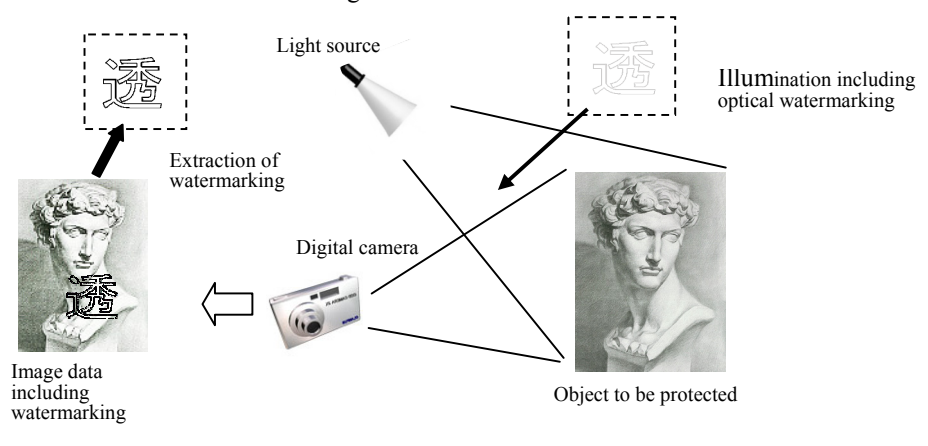


Fig. 1. Basic concept underlying proposed technology

it is applied to 2D objects. This paper describes our experiments on a method of extracting embedded watermarking data from captured images of 3D objects, and presents results that demonstrate the feasibility of optical watermarking technology applying to 3D objects.

II. WATERMARKING TECHNIQUE APPLYING TO BASIC 2D OBJECTS

Fig. 1 outlines the basic concept underlying the optical watermarking technology. The light source contains the watermarking information and illuminates an object. A projector is possibly used as the light source that provides a distribution of 2D-illumination. The brightness of the object's surface is proportional to the product of the reflectance of the surface and the illumination by the light source that includes the invisible watermarking image.

Fig. 2 illustrates the procedure for watermarking using orthogonal transforms. The watermarking area is divided into units of 16×16 or 8×8 pixel blocks, and each block has a DC component that gives an average brightness for the entire watermarking area, i.e., the brightness of illumination. Every block also has the highest frequency component (HC) in both the x- and y- directions to express the 1-bit binary information for watermarking. The phase of HC was used to express binary data i.e., "0" or "1". Two orthogonal transforms were used to produce the watermarking images. The first was a 2D inverse DCT (i-DCT), which is

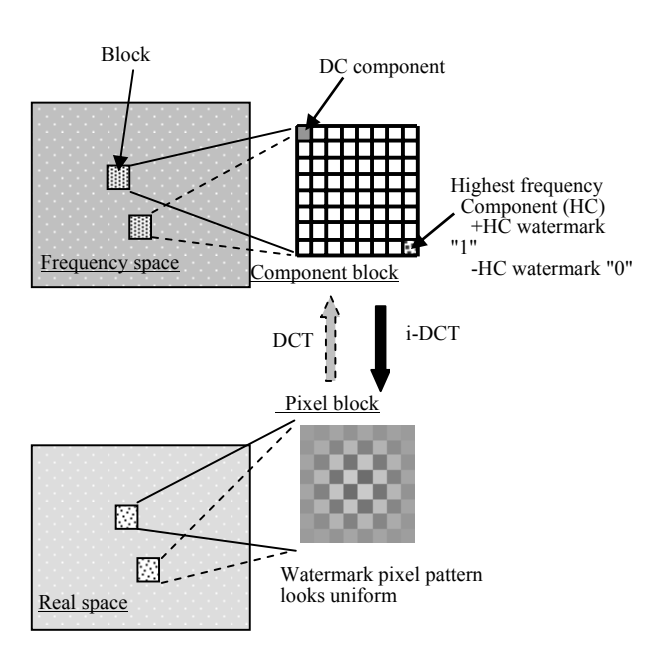


Fig. 2. Producing watermarks

mathematically expressed with Eq. (1).
$$f_{i,j}(x,y) = \sum_{u}^{N-1} \sum_{v}^{N-1} C(u)C(v)F_{i,j}(u,v)\cos\{\frac{(2x+1)u\pi}{2N}\}\cos\{\frac{(2y+1)v\pi}{2N}\}$$
 (1)

where $f_{i,j}(x,y)$ are the watermarking image data for pixel (x,y) of block (i,j) in real space, $F_{i,j}(u,v)$ are the data for component (u,v) of block (i,j) in frequency space, and N is the number of pixels in the block in the x- and y-directions. Here, C(u) and C(v) are given as

$$C(u) = \begin{cases} 1 & (u = 0) \\ \sqrt{2} & (u \neq 0) \end{cases}, \qquad C(v) = \begin{cases} 1 & (v = 0) \\ \sqrt{2} & (v \neq 0) \end{cases}$$

Table 1. Walsh-Hadamard Matrix

(a) 8×8 Matrix

		_	_	_	_	_	_
1	1	1	1	1	1	1	1
1	1	1	1	-1	-1	-1	-1
1	1	-1	-1	-1	-1	1	1
1	1	-1	-1	1	1	-1	-1
1	-1	-1	1	1	-1	-1	1
1	-1	-1	1	-1	1	1	-1
1	-1	1	-1	-1	1	-1	1
1	-1	1	-1	1	-1	1	-1

(b) 16×16 Matrix

1	1	1	1	1	1	1	1	1	1	1	1	1	1	1	1
1	1	1	1	1	1	1	1	-1	-1	-1	-1	-1	-1	-1	-1
1	1	1	1	-1	-1	-1	-1	-1	-1	-1	-1	1	1	1	1
1	1	1	1	-1	-1	-1	-1	1	1	1	1	-1	-1	-1	-1
1	1	-1	-1	-1	-1	1	1	1	1	-1	-1	-1	-1	1	1
1	1	-1	-1	-1	-1	1	1	-1	-1	1	1	1	1	-1	-1
1	1	-1	-1	1	1	-1	-1	-1	-1	1	1	-1	-1	1	1
1	1	-1	-1	1	1	-1	-1	1	1	-1	-1	1	1	-1	-1
1	-1	-1	1	1	-1	-1	1	1	-1	-1	1	1	-1	-1	1
1	-1	-1	1	1	-1	-1	1	-1	1	1	-1	-1	1	1	-1
1	-1	-1	1	-1	1	1	-1	-1	1	1	-1	1	-1	-1	1
1	-1	-1	1	-1	1	1	-1	1	-1	-1	1	-1	1	1	-1
1	-1	1	-1	-1	1	-1	1	1	-1	1	-1	-1	1	-1	1
1	-1	1	-1	-1	1	-1	1	-1	1	-1	1	1	-1	1	-1
1	-1	1	-1	1	-1	1	-1	-1	1	-1	1	-1	1	-1	1
1	-1	1	-1	1	-1	1	-1	1	-1	1	-1	1	-1	1	-1

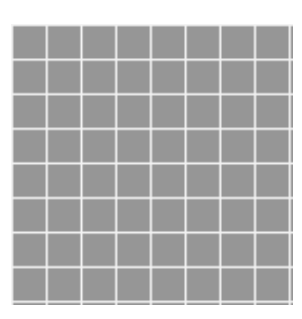
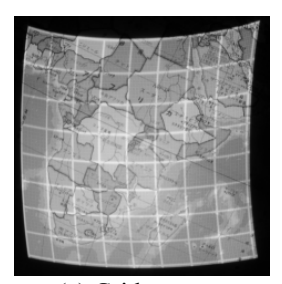
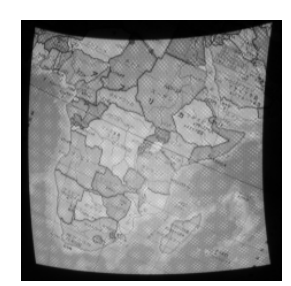


Fig.3. Grid pattern image used in experiments



(a) Grid pattern

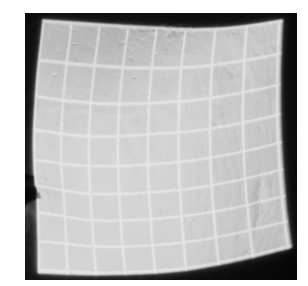


(b) Watermarking image

Fig.4. Photograph of globe on which image was projected



(a) Human-face model



(b) Magnified image of grid pattern



(c) Magnified image of watermarking area

Fig.5. Photograph of human-face model on which watermark image was projected

The second was a 2D inverse WHT (i-WHT), which is expressed by Eq. (2).

$$f_{i,j}(x,y) = \frac{1}{N} \sum_{u=1}^{N-1} \sum_{v=1}^{N-1} F_{i,j}(u,v) w h(x,u) w h(v,y)$$
 (2)

where wh(i, j) denotes a component of the Walsh-Hadamard matrix in Table 1.

In both methods, $F_{i,j}(u,v)$ is given as

$$F_{i,j}(0,0) = DC$$
 (3)

$$F_{i,j}(N-1,N-1) =$$

HC, if binary data to be embedded in block (i, j) are "1" -HC, if binary data to be embedded in block (i, j) are "0"

$$F_{i,j}(u,v) = 0$$
 (for $u, v \neq 0$, N-1) (5)

Eqs. (3)-(5) indicate that the produced image only has the DC component and HC, and the other components are set to "0". Therefore, the embedded watermarking image projected onto the object using a projector could hardly be seen by the human-visual system but it could be easily read out from the object image. Because the frequency components of the object image itself were lower than the HC, the embedded information for watermarking was easily separated from the object image.

III. APPLYING TO 3D OBJECTS

First, the grid pattern image that divides the region of the optical watermarking equally into 8×8 is irradiated onto the object image (Fig. 3) and captured with a digital camera to apply optical watermarking technique to 3D objects. The coordinates of the corner points of the segmented areas are measured respectively on the captured image data. Then, the

image data irradiated with optical watermarking are captured, and these are corrected by using the coordinates of the corner points of the segmented area as each segmented region may become a precise square.

The transformation from an undistorted coordinate system (x, y) to a geometrically distorted system (x', y') is generally expressed by following equations.

$$x' = h_1(x, y), \quad y' = h_2(x, y)$$
 (6)

If the distortion is perspective, the transformation is expressed by the following linear equations.

$$x' = ax + by + d$$
, $y' = dx + ey + f$ (7)

The shape of the image containing the generated watermark is a precise rectangle, and all areas divided with an 8×8 grid pattern are also precise rectangles. However, if these were

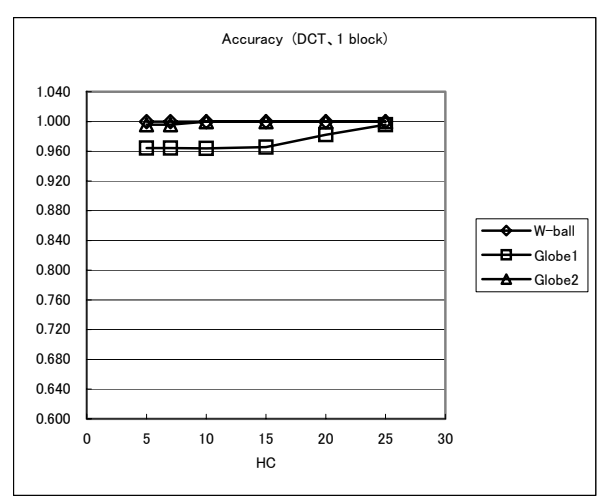


Fig. 6. (a) Accuracy with which data were read out: Whiteball and Globe (DCT, one block evaluation)

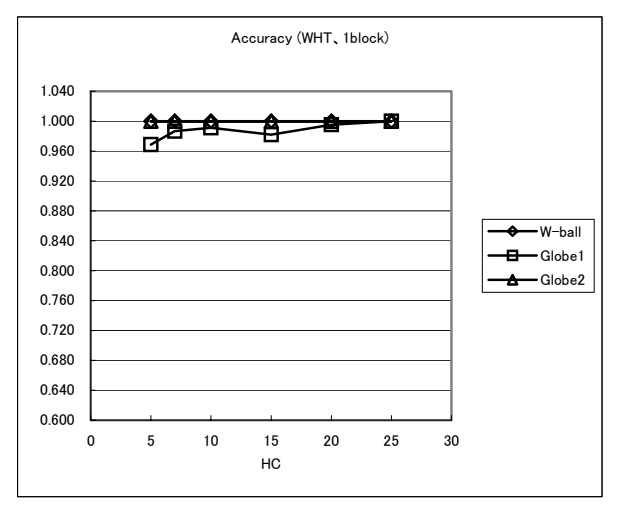


Fig. 6. (c) Accuracy with which data were read out: Whiteball and Globe (WHT, one block evaluation)

distorted in perspective, they become general quadrangles. When the coordinates of all corner points of a quadrangle are given, the coefficients of the above-mentioned linear equations can be determined from three of these and the corresponding coordinates of the original undistorted rectangle. Using these equations the value of pixels in the distorted quadrangle can be transformed to the value of pixels in the undistorted rectangle. However, because the coordinates of transformed pixels do not generally become integers, an interpolation technique is utilized to determine the density value of the nearest pixel. Linear transformation using the four nearest neighboring pixels was used in the experiments, which is so called "bi-linear interpolation" [6].

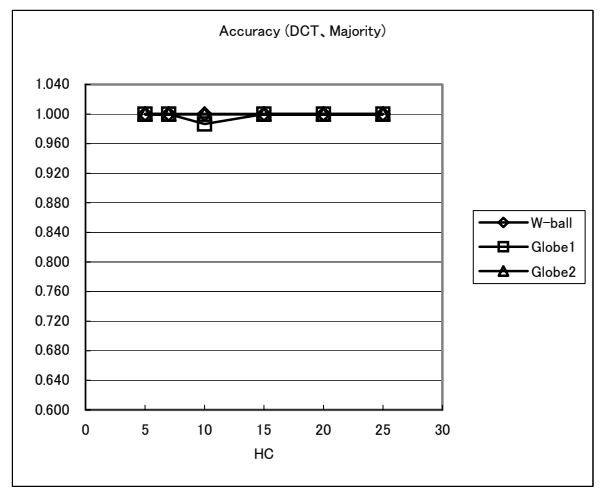


Fig. 6. (b) Accuracy with which data were read out: White-ball and Globe (DCT, Majority evaluation)

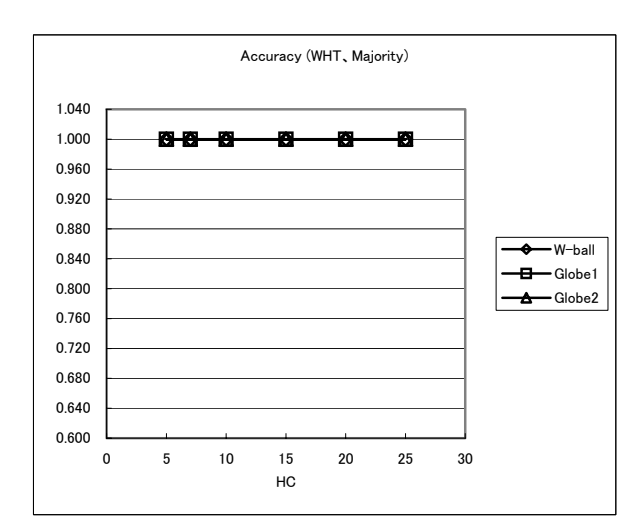


Fig. 6. (d) Accuracy with which data were read out: White-ball and Globe (WHT, Majority evaluation)

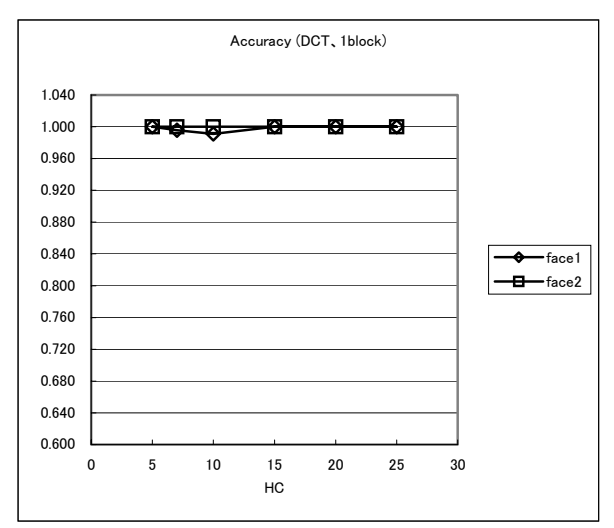


Fig. 7. (a) Accuracy with which data were read out: Human-face model (DCT, one block evaluation)

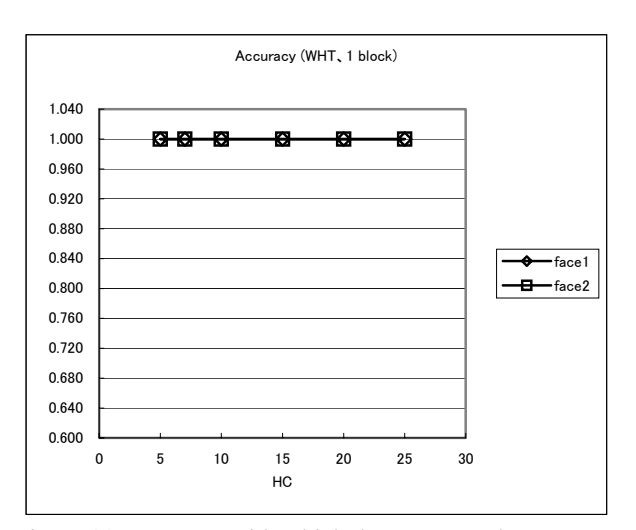


Fig. 7. (c) Accuracy with which data were read out: Human-face model (WHT, one block evaluation)

IV. EXPERIMENTS

Watermarking images that consisted of 16×16 blocks were produced in the experiments. Each block had 8×8 pixels, i.e., the watermarking images had 128×128 pixels. A Digital Light Processing (DLP) projector that had a resolution of 800×600 pixels was used as a light source. The watermarking images were projected onto objects, which were a white hemisphere, a globe, and a model of a human face. As previously mentioned, the image of a grid pattern (divided into 8×8) was first irradiated onto objects and the coordinates of the grid points were measured manually using the grid pattern. A watermarking image was next irradiated and image data were captured with a digital camera. Fig. 4. (a) shows the image of a globe that was irradiated with the

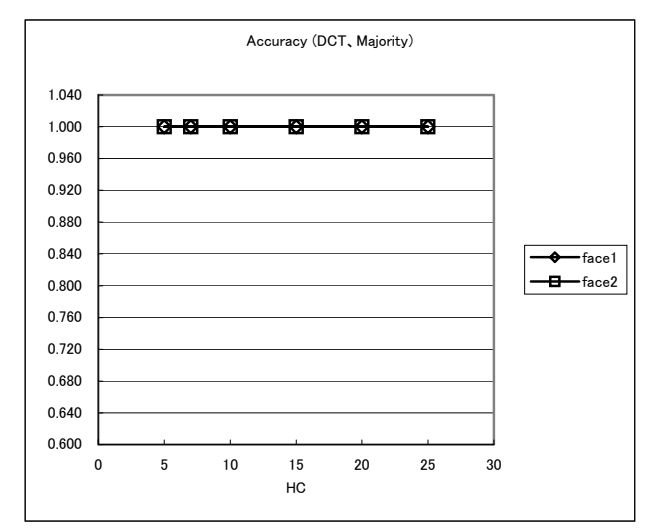


Fig. 7. (b) Accuracy with which data were read out: Human-face model (DCT, Majority evaluation)

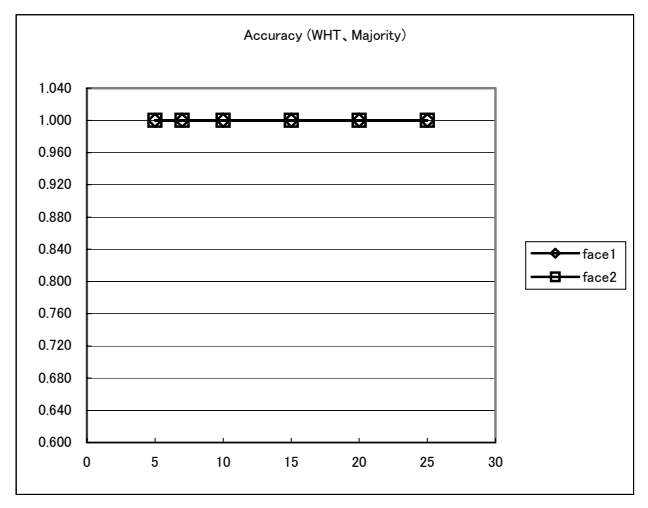


Fig. 7. (d) Accuracy with which data were read out: Human-face model (WHT, Majority evaluation)

grid pattern image, and Fig. 4. (b) has the image of a globe that was irradiated with a digital watermarking image. Figs. 5. (a)-(c) also show photographs of the human-face model onto which the watermarking image or grid pattern image was projected.

Using the measured coordinates of the grid points, the whole distorted rectangle was clipped out from the captured image data and at the same time 8×8 divided domains were identified in the clipped out area. Then, each of the 8×8 domains was corrected to a precise rectangle with the method of correction described in the previous section. The resolution of the restored rectangular area was about 650×650 pixels using a digital camera with a resolution of 4288×2848 pixels. It was then transformed to just 256×256 pixels and divided into 16×16 blocks, each of which had 16×16 pixels. We

also carried out DCT on all blocks using Eq. (8),

$$F_{i,j}(u,v) = \frac{C(u)C(v)}{M \times M} \sum_{x}^{M-1} \sum_{y}^{M-1} f_{i,j}(x,y) \cos\left\{\frac{(2x+1)u\pi}{2M}\right\} \cos\left\{\frac{(2y+1)v\pi}{2M}\right\}$$
(8)

We also utilized Eq. (9) for WHT, using the values in Table 1(b) as the components of matrix wh(i, j).

$$F_{i,j}(u,v) = \frac{1}{M} \sum_{n=1}^{M-1} \sum_{x=1}^{M-1} f_{i,j}(x,y) wh(u,x) wh(y,v)$$
(9)

where M is the number of pixels in the u and v directions in frequency space, which was 16 in the experiments.

The accuracy with which the embedded data were read out was evaluated by checking the sign of the $F_{i,j}(7,7)$ components for all blocks. Two methods of embedding data were used. The "1-block method" involved embedding 1-bit data into one block and embedding 256 1-bit binary data into 16×16 blocks. The "majority method" involved embedding the same 1-bit data into three blocks sufficiently separated from one another, and it was used to determine the readout data by using the majority decision. The distance between the blocks was set to five and 75 1-bit binary data were embedded in 16×16 blocks in the experiments.

V. RESULTS AND DISCUSSION

Figs. 6. (a) - (d) plot the results of irradiating the optical watermarking created for a white hemisphere and a globe (European-African hemisphere and Pacific-Ocean hemisphere) with DCT and WHT, and measuring the rate at which watermark information was detected. The results of evaluating accuracy for the white hemisphere had 100% under all conditions with DCT and WHT. However, 100% accuracy was not achieved in evaluating accuracy with the globe, especially in the European-African hemisphere, where the 1-bit block method was used with DCT and WHT. The decision by using the majority method achieved an accuracy of 100% excluding the HC=10 of DCT. The European-African hemisphere has numerous black lines and characters and these could disturb the accuracy of reading out embedded

Figs.7. (a) - (d) indicate an accuracy of 100% for the evaluation of the human-face model under all conditions in the decision by the majority method. The 1- block method achieved an accuracy of 100% excluding part of the DCT. The surface of the face model was painted white in this experiment, and the reflectivity of the surface may have been proportional to the brightness of the irradiated optical watermarking.

We concluded from these results that the geometrical distortion of a 2D image irradiated onto the curved surface of a 3D object could be restored with a very high degree of accuracy if the method of rectangular mesh fitting and the "bi-linear interpolation" technique based on the nearest four points were used.

VI. CONCLUSION

We proposed the application of optical watermarking to 3D objects, which can prevent sculptures in museums, for example, from being illegally photographed. We used methods of correcting distortions in captured images caused by projecting optical watermarking image onto the curved surface of objects. We found that the embedded data were read out with almost 100% accuracy when DCT and WHT were used for embedding watermarking, after distortions in the captured images had been corrected by using a method that involved a grid pattern.

This paper discussed a method of correcting distortions using a projected grid image to indicate the correct pixel block, prior to the images for embedding watermarking being captured. However, if a marker is also embedded into optical watermarking images, it can easily be extracted with image processing. For example, if a grid pattern image and a watermarking image have different colors and are embedded simultaneously, they can easily be separated from each other. Therefore, geometrical distortions in optical watermarking images due to them being projected onto 3D objects can easily be removed. We demonstrated the feasibility of using optical watermarking technique to protect objects from being illegally captured which has been difficult to accomplish with conventional watermarking technology.

REFERENCES

- I. J. Cox, J. Kilian, F. T. Leighton and T. Shamoon, "Secure spread spectrum watermarking for multimedia", IEEE Trans. Image Process., Vol. 6, No. 12, pp. 1673-1687 (1997)
- [2] M. D. Swanson, M. Kobayashi and A. H. Tewfik, "Multimedia dataembedding and watermarking technologies", Proc. IEEE, Vol. 86, No. 6, pp. 1064-1087 (1998).
- [3] M. Hartung and M. Kutter, "Multimedia watermarking techniques", Proc IEEE, Vol.87, No.7, pp.1079-1107 (1999)
 [4] T. Mizumoto and K. Matsui, "Robustness investigation of DCT digital
- [4] T. Mizumoto and K. Matsui, "Robustness investigation of DCT digital watermark for printing and scanning", Trans. IEICE (A), Vol. J85-A, No. 4, pp. 451-459 (2002)
- [5] M. Ejima and A. Miyazaki, "Digital watermark technique for hard copy image", Trans. IEICE (A), Vol. J82-A, No. 7, pp. 1156-1159 (1999)
- [6] A. Rosenfeld and A. C. Kak, Digital Picture Processing. New York: Academic Press, pp. 175-179 (1976).